

Photoluminescence Studies of ZnO, ZnO:Eu and ZnO:Eu Nanoparticles Covered with Y₂O₃ Matrix

Laishram Robindro Singh

Department of Nanotechnology, North-Eastern Hill University, Shillong, India
Email: lsingh@nehu.ac.in

Received 3 March 2015; accepted 26 March 2015; published 27 March 2015

Copyright © 2015 by author and Scientific Research Publishing Inc.
This work is licensed under the Creative Commons Attribution International License (CC BY).
<http://creativecommons.org/licenses/by/4.0/>



Open Access

Abstract

Development of advanced display and lighting technology such as field emission displays and plasma display panels requires phosphor which has a high efficiency and low degradation. Particle sizes and the locations of dopants in the hosts take an important role in the luminescence emissions of phosphors. ZnO nanoparticles are widely employed in plasma field emission display devices and well investigated; however, lanthanide (Ln³⁺) doped ZnO needs more investigations. In ZnO:Eu the lanthanide ions (Eu³⁺) may occupy either Zn²⁺ lattice site or on surface of ZnO crystal. The emissions of Eu³⁺ ion on the surface are the characteristic of Eu₂O₃, which leads to weak luminescence emission. To observe such phenomena, nanoparticles of ZnO, 2 at.% Eu³⁺ doped ZnO (ZnO:Eu) and ZnO:Eu covered with yttria matrix were prepared by wet chemical method at low temperature. The prepared nanoparticles were characterized by XRD and TEM. XRD data reveal the significant phase segregation of the annealed nanoparticles compared with lower heated samples. This phase segregation of Eu³⁺ ion establishes responsible for the decrease luminescence intensity of annealed ZnO:Eu nanoparticles compared with the as-prepared ZnO:Eu nanoparticles. Improvement on luminescence emissions could be achieved only for the as-prepared ZnO:Eu nanoparticles while covered with yttria matrix.

Keywords

Nanoparticles, Phase Segregation, Dispersion, Luminescence, Core-Shell

1. Introduction

ZnO is a direct band gap semiconductor of band gap 3.2 eV at room temperature and one of the potential mate-

rials in various display devices [1] [2]. Luminescent properties of ZnO can be improved by doping ZnO with transition metals or lanthanide ions. Extensive luminescence studies have been carried out some of the systems like ZnO:Eu, ZnO:Mn, ZnO:V, ZnO:W etc. [3]-[7], since the last three decades. As the luminescent properties of Eu^{3+} ions in different crystallographic environments are well understood, it can be used as a probe to monitor the structural changes taking place around it, when doped in different inorganic materials. Among them, luminescent properties of ZnO:Eu system have been investigated by a number of authors [3]-[7] keeping in mind its potential applications as materials in field emission display devices. Our previous luminescence studies of ZnO:Eu nanoparticles showed that there were no energy transfer between the host ZnO and Eu^{3+} ions [8]. As the Eu^{3+} ions have very poor solubility in ZnO, most of the Eu^{3+} ions are lying on the surface of the ZnO particles, only few ions may be in the lattice site while annealing at high temperature results migration of Eu^{3+} ions towards the grain boundaries (distorted environment) and segregation of Eu^{3+} into separate Eu_2O_3 phase. Both the phenomena produce significant reduction of their luminescent properties. Hence low temperature synthesis will be suitable Eu^{3+} doped ZnO nanoparticles. Low temperature synthesis normally leads to smaller particle size. One way to circumvent this problem is to cover the surface of the nanoparticles with suitable inorganic materials or dispersion in organic/inorganic materials wherein the Eu^{3+} ions can migrate without phase separation. Y_2O_3 turned out to be a suitable choice as it was a suitable host for the lanthanide ions. Shell formation with Y_2O_3 , it is expected that there will not have any nanoparticle aggregation and phase separation of Eu_2O_3 .

In this article, ZnO:Eu and ZnO:Eu nanocrystals covered with yttria matrix (ZnO:Eu/ Y_2O_3) prepared at low temperature (140°C) and critical luminescence studies were also carried out for ZnO, ZnO:Eu and ZnO:Eu/ Y_2O_3 nanoparticles of different particle sizes.

2. Experimental

2.1. Preparation

Nanoparticle of ZnO, 2 at.% Eu^{3+} doped ZnO (ZnO:Eu), ZnO:Eu covered with in Y_2O_3 (ZnO:Eu/ Y_2O_3) were prepared by wet chemical in polyethylene glycol medium at 140°C . The preparation procedures were similar to our earlier reports [8]-[10]. To prepare ZnO:Eu covered with in Y_2O_3 , 98 at.% Zn^{2+} , 2 at.% Eu^{3+} and 100 at.% Y^{3+} were used, the precursors used for production of Zn^{2+} , Eu^{3+} and Y^{3+} are $\text{Zn}(\text{CH}_3\text{COO})_2 \cdot 2\text{H}_2\text{O}$ (99.05%, E-Merck), Eu_2O_3 (99.99% Aldrich) and $\text{Y}_2(\text{CO}_3)_3 \cdot 3\text{H}_2\text{O}$ (99.99%, Alfa Aesar) respectively. Polyethylene glycol acts as reaction medium as well as the capping agent during the preparation process. To prepare ZnO doped with 2 at.% Eu^{3+} , 0.50 g of $\text{Zn}(\text{CH}_3\text{COO})_2 \cdot 2\text{H}_2\text{O}$ was dissolved in 50 ml of polyethylene glycol mixture (form by 80:20 ratio of polyethylene and ethylene glycol), warm the mixture at 60°C within few minutes a clear solution could be observed. Then, 0.00734 g of Eu_2O_3 dissolved in dil-HCl, warmed the solution several times in double distilled water to get rid out excess acids from the solution. This solution containing Eu^{3+} ions were simply mixed to the above solution. Another solution containing 0.2 M of NaOH (Merk-GR) was made and simply added to the above mixtures then heated linearly up to 140°C . The reaction temperature was maintained for one hour. A cloudy white precipitate could be observed and the reaction continued another two hours. The precipitate so obtained was extracted by centrifugation. The powder so obtained were the ZnO:Eu nanoparticles. In the second step, to cover ZnO:Eu nanoparticles with Y_2O_3 matrix, the former solution containing ZnO:Eu refluxed again simply by addition of another solution containing Y^{3+} (to get Y^{3+} , 0.4785 g of $\text{Y}_2(\text{CO}_3)_3 \cdot 3\text{H}_2\text{O}$ dissolve in dil-HCl, warm the solution several times in excess double distilled water). Further 20 ml solution of 0.2 M strength of NaOH added to the above mixture then heated slowly at the same reaction temperature. A thick milky white precipitate could be obtained, the reaction continues another three hours, the precipitate so obtained was extracted by centrifugation in excess ethanol. This powder sample was the ZnO:Eu/ Y_2O_3 nanoparticles. The powder samples so obtained were dried for further characterization and luminescence measurements.

2.2. Characterization

X-ray diffraction studies were carried out using a Philips powder X-ray diffractometer (model PW 1071) with Ni filtered Cu-K_α radiation. The lattice parameters were calculated from the least square fitting of the diffraction peaks. The average crystallite size was calculated from the diffraction line width based on Scherrer relation: $d = 0.9\lambda/B\cos\theta$, where λ is the wavelength of X-rays and B is the half maximum line width.

All luminescence measurements were carried out at room temperature with a resolution of 3 nm, using a Hi-

tachi Instrument (F-4500) having a 150 W Xe lamp as the excitation source. Powder samples were mixed with methanol, spread over a quartz plate, dried at 100°C and mounted inside the sample chamber. All Transmission Electron Microscopy (TEM) images are done using CM 200 Phillips.

3. Results and Discussion

3.1. XRD and TEM Study

Figure 1(a) shows the XRD patterns of as-prepared ZnO and **Figures 1(b)-(d)** gives the XRD pattern of as-prepared 2 at.% Eu^{3+} doped ZnO (ZnO:Eu) nanoparticles along with their 500°C and 900°C heated samples. The particles are crystalline with hexagonal structure with S. G. $P6_{3mc}$, all the diffraction peaks corresponds to the JCPDS 36-1451. No other characteristic peaks of europium impurity such as Eu_2O_3 could be detected at least within the resolution limit of the diffractometer. The broadening of the diffraction peaks are the characteristic of nanosized ZnO materials. The lattice parameters of as-prepared sample are found to be $a = 3.249(1) \text{ \AA}$ and $c = 5.205(1) \text{ \AA}$. Bulk value of ZnO has lattice parameters $a = 3.249 \text{ \AA}$, $c = 5.206 \text{ \AA}$ (JCPDS 36-1451). Lattice parameters are close to bulk value. The crystallite sizes are calculated from the peak position of ZnO:(101) plane. The crystallite size of as-prepared sample is found to be 12 nm. With Eu^{3+} incorporation, there is slight shift in the diffraction peak maxima towards lower 2θ values compared to as-prepared ZnO (**Figure 1(b)**), indicating the lattice expansion of the host lattice with Eu^{3+} incorporation. The lattice parameter values are found to be $a = 3.254(1)$, $c = 5.208(1) \text{ \AA}$. It is understandable as the ionic radius of Eu^{3+} (0.95 Å) is higher than that of Zn^{2+} (0.70 Å) and hence the Eu^{3+} incorporation in the ZnO lattice is associated with lattice expansion. It may be quite possible that many of the Eu^{3+} ions must be occupying the Zn^{2+} lattice site of ZnO nanoparticles. Annealing the samples at 500°C and 900°C result in the slight shifting of the diffraction peaks to higher 2θ values, revealing that the lattice parameter decrease with increase in heat treatment temperatures. The lattice parameters of 500°C heated sample are $a = 3.252(1) \text{ \AA}$ and $c = 5.208(1) \text{ \AA}$, and for 900°C heated sample the corresponding values are $a = 3.249(1) \text{ \AA}$ and $c = 5.207(1) \text{ \AA}$ respectively. From these results it can be confirmed that there are partial removal of Eu^{3+} ions from the ZnO lattice with heat treatment. The crystallite sizes are calculated from the peak position of ZnO:(101) plane by Gaussian fitting. The crystallite sizes of 2 at.% Eu^{3+} doped ZnO (ZnO:Eu) nanoparticles: as-prepared, 500°C and 900°C heated samples are 8, 16 and 36 nm respectively suggesting the agglomeration of particles on higher heat-treatment.

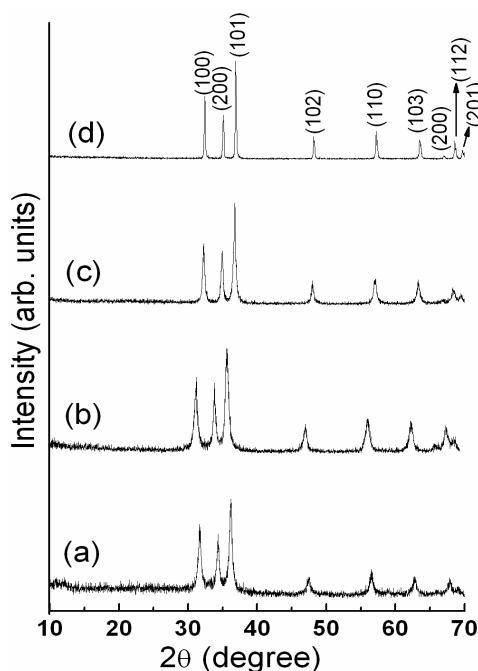


Figure 1. XRD patterns of (a) as-prepared ZnO, (b) 2 at.% Eu doped ZnO and heat-treated ZnO (c) at 500°C and (d) at 900°C.

Figures 2(a)-(c) show XRD patterns of as-prepared 2 at.% Eu^{3+} doped ZnO (ZnO:Eu) nanoparticles covered with in Y_2O_3 (ZnO:Eu/ Y_2O_3) along with their 500°C and 900°C heated samples. In as-prepared sample only the characteristic peaks of ZnO could be observed indicating that Y_2O_3 phases are amorphous. However on heating the samples at 500°C and 900°C, along with diffraction peaks characteristic of ZnO the characteristic peaks of cubic Y_2O_3 are also appeared. The * indicates the characteristics peaks of Y_2O_3 phases. The crystallite sizes are calculated from the peak position of ZnO:(101) plane. The crystallite sizes of 2 at.% Eu^{3+} doped ZnO (ZnO:Eu) nanoparticles covered with Y_2O_3 are 8, 13 and 32 nm respectively for the as-prepared, 500°C and 900°C heated samples, indicating the increase of particle size with heat-treatment. The lattice parameters of ZnO present in ZnO:Eu/ Y_2O_3 are $a = 3.256(1) \text{ \AA}$, $c = 5.208(1) \text{ \AA}$ for as-prepared sample and for the 500°C and 900°C heat-treated samples are $a = 3.251(1) \text{ \AA}$, $c = 5.208(1) \text{ \AA}$ and $a = 3.249(1) \text{ \AA}$, $c = 5.208(1) \text{ \AA}$ for 900°C respectively. Bulk value of ZnO has lattice parameters $a = 3.249 \text{ \AA}$, $c = 5.206 \text{ \AA}$, and volume, $V = 47.62 \text{ \AA}^3$. It suggests that lattice parameters decreases with the heat-treatment indicating Eu^{3+} coming out from ZnO lattice with heat-treatment. The lattice parameter and unit cell volume of Y_2O_3 present in ZnO:Eu/ Y_2O_3 are $a = 10.621(1) \text{ \AA}$ for 500°C heat-treated sample; and $a = 10.649(1) \text{ \AA}$ for 900°C heat-treated sample. The lattice parameters for the bulk value of Y_2O_3 is $a = 10.604 \text{ \AA}$, and volume, $V = 1192.40 \text{ \AA}^3$ [11]. Unit cell parameter of Y_2O_3 in ZnO:Eu/ Y_2O_3 samples increase with heat-treatment. It indicates that Eu^{3+} ions which are coming out from the ZnO lattice diffuse into Y_2O_3 lattices occupying Y^{3+} sites.

TEM picture shows the as-prepared ZnO:Eu nanoparticles are in spherical shape covered with Y_2O_3 particles (ZnO:Eu/ Y_2O_3), the particle size is found to be 13 nm as shown in **Figure 3(a)**. The bright portion shows the ZnO:Eu nanoparticles surrounded by dark Y_2O_3 particles. The inset figure shows the expansion of it, showing ZnO particles are covered with Y_2O_3 particles. **Figure 3(b)** shows the TEM picture of 900°C treated ZnO:Eu/ Y_2O_3 nanoparticles. It shows that both the ZnO and the Y_2O_3 particles are crystalline, though Y_2O_3 fairly covered to ZnO:Eu particles. The particle size is 46 nm. The particle sizes determined by XRD and TEM are in agreement.

3.2. Luminescence Study

Figure 4 shows the emission spectra of pure (a) as-prepared, (b) 500°C and (b) 900°C heat-treated ZnO nanoparticles excited at 320 nm. In as-prepared sample the pattern consists of a sharp peak around 390 nm superimposed over a broad peak centered around 500 nm. Weak luminescence emission at 465 nm could be detected in this sample. Based on the previous photoluminescence studies of ZnO nanoparticles [12]-[14], the peak around

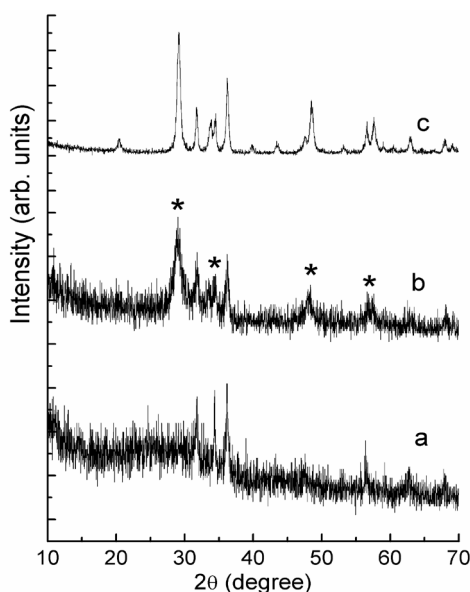


Figure 2. XRD pattern of 2 at.% Eu doped ZnO nanoparticles dispersed in Y_2O_3 (a) as-prepared, (b) 500°C and (c) 900°C heat-treated nanoparticles, the * shows the Y_2O_3 phase in the pattern.

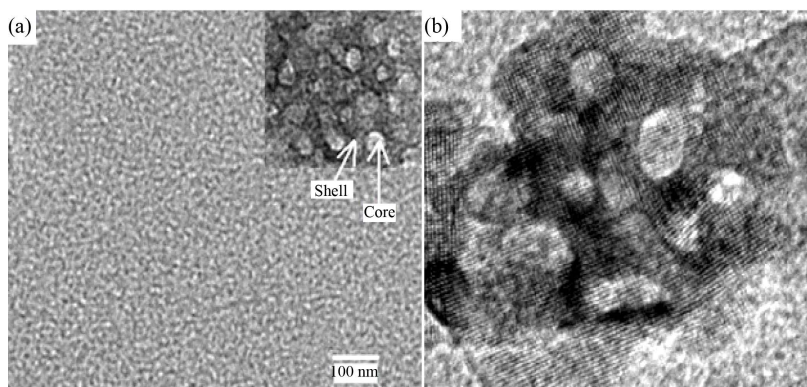


Figure 3. TEM images of (a) as-prepared 2 at.% Eu doped ZnO nanoparticles covered with Y_2O_3 along with its expansion in the inset and (b) shows the 900°C heat-treated ZnO:Eu/ Y_2O_3 nanoparticles.

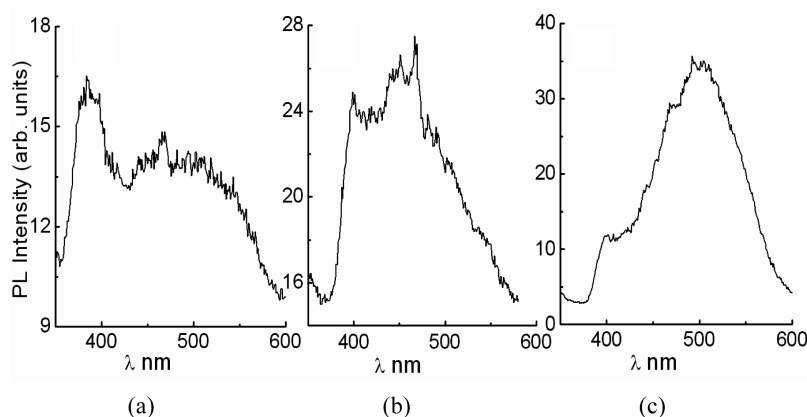


Figure 4. Photoluminescence emission spectra of (a) as-prepared and heat-treated at (b) 500°C and (c) 900°C ZnO nanoparticles excited at 320 nm.

390 nm has been attributed to the near band edge emission due to the exciton emission [12], that of 465 nm emission is due to excitons on the surface of ZnO nanoparticles and that around 500 nm has been attributed to the defects present in the ZnO lattice or the deep level electrons [11]-[18]. In 500°C heat-treated sample the emission at 466 nm is dominant over the 390 and 500 nm emissions, this emission is due to the native defect of ZnO nanoparticle or the emission due to surface trap excitons. For the sample heat-treated at 900°C, the green emission around 500 nm is dominated over the band edge emission 390 nm and that of surface trap emission 466 nm. The green emission of ZnO is still on debate [17]-[23], but in our observation this emission is due to oxygen vacancy [10]. In order to confirm the exact peak positions of luminescence emissions, the photoluminescence emission spectrum of 900°C heat-treated ZnO nanoparticle is deconvoluted with Gaussian fitting (chi square = 0.9988) as shown in Figure 5. It is observed two peaks centered at 390 and 504 nm. The emission of native defect state could not be detected. It is observed that the UV-emission and the visible light emissions of ZnO nanoparticles depend on the particle size. With incorporation of Eu^{3+} in the ZnO lattice, no defect or exciton emissions could be observed. However strong Eu^{3+} emissions due to the transition $^5D_0 \rightarrow ^7F_1$ (orange emission at 590 nm) and $^5D_0 \rightarrow ^7F_2$ (yellow emission at 615 nm) could be observed on direct excitation of Eu^{3+} ion at 394 nm ($^7F_0 \rightarrow ^5L_6$) as shown in Figure 6(a). Heating the sample at 500°C there is significant reduction in the Eu^{3+} luminescent intensity as seen from Figure 6(b) and on further heating at 900°C no emission could be observed from the sample (Figure 6(c)). Partial phase segregation of Eu^{3+} ions as well as Eu^{3+} incorporation in the grain boundaries (distorted regions) are responsible for the significant reduction in the luminescence intensity of heated samples. These results are supported by XRD data, decreased in the lattice parameter values of the ZnO:Eu nanoparticles for higher heat-treatments at 500°C and 900°C. It is worth to mention, even though the luminescence emission intensities decrease with the raise heat-treatment temperatures, the peak positions of the emission lines

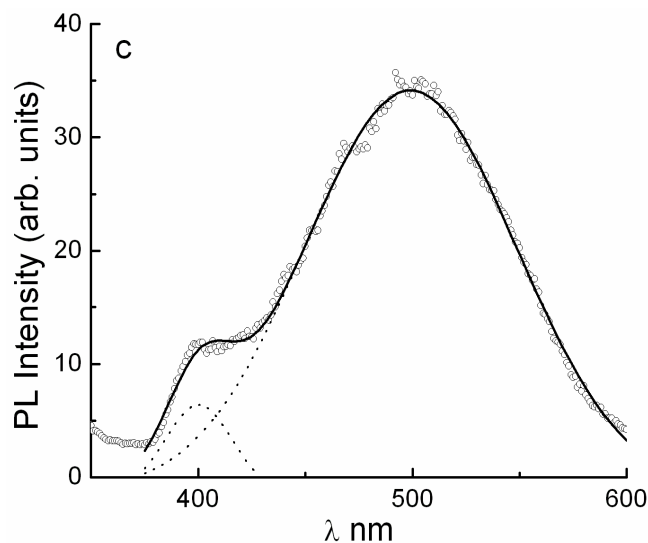


Figure 5. Deconvolution of 900°C heat-treated ZnO nanoparticle, ooo signifies the experimental data, — indicates the fitted curve and the indicates the deconvoluted curves.

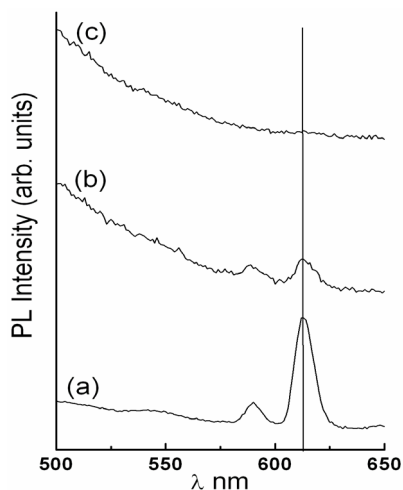


Figure 6. Photoluminescence emission spectra of ZnO:Eu nanoparticles (a) as prepared and its (b) 500°C and (c) 900°C heat treated samples excited at $f-f$ transition of Eu^{3+} ion (394 nm).

do not change *i.e.* the emission lines are still at 615 nm.

Figure 7 shows the emission spectra corresponding to as-prepared ZnO:Eu/Y₂O₃ nanoparticles along with their heat-treatments at 500°C and 900°C. There are two strong emission lines due to $f-f$ transitions of Eu^{3+} ions at $^5\text{D}_0 \rightarrow ^7\text{F}_1$ and $^5\text{D}_0 \rightarrow ^7\text{F}_2$. Here opposite phenomena could be observed compared to heat-treated ZnO:Eu nanoparticles, strong emission peaks of Eu^{3+} ions could be detected for the heat-treated ZnO:Eu/Y₂O₃ samples and luminescence intensity also increased with the increase heat-treatment temperature. It also observes in the emission lines that the peak positions of the heat-treated samples are shifting towards lower wavelength side (at 610 nm) compared to the as-prepared sample (remain at 615 nm). Why such phenomena could be observed in the emission spectra of ZnO:Eu/Y₂O₃ samples? It is clearly observed the luminescence emission intensity of as-prepared ZnO:Eu/Y₂O₃ is at 615 nm and strong. In the as-prepared ZnO:Eu/Y₂O₃ sample, Y₂O₃ exists as amorphous as revealed by the XRD data in **Figure 2**. The emission lines of ZnO:Eu/Y₂O₃ nanoparticles are from the ZnO:Eu particles, not from Y₂O₃. In such samples the Y₂O₃ is amorphous that is Y(OH)₃, the Eu^{3+} ions occupy the Zn^{2+} site in ZnO and results the emission lines. If the emissions are from Y₂O₃, it will be from surface

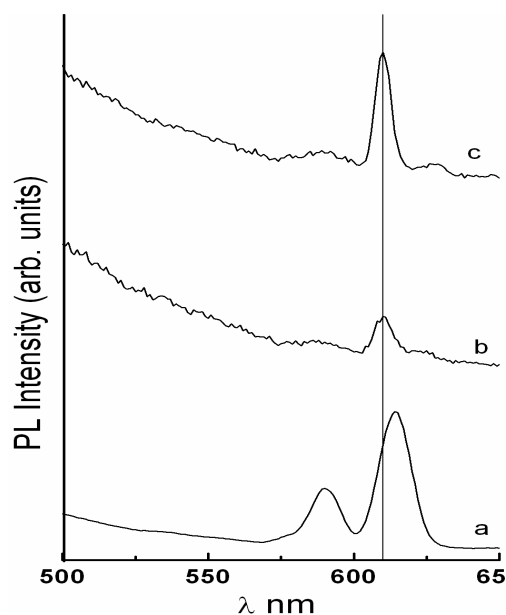


Figure 7. Photoluminescence emission spectra of ZnO:Eu nanoparticles covered with Y_2O_3 (a) as-prepared, (b) $500^\circ C$ and (c) $900^\circ C$ heat-treated samples excited at $f-f$ transition of Eu^{3+} (394 nm).

ions *i.e.* Eu^{3+} ions by forming weakly bonded Eu_2O_3 and will be leading weak luminescence emission from such particles [9]. To confirm these emissions are either from ZnO:Eu or $Y(OH)_3$ particles, 2 at.% of Eu^{3+} ion doped Y_2O_3 was prepared at the same reaction temperature (the preparation procedure was similar to LR Singh *et al.* [9] except using NaOH in place of urea). Comparison of luminescence emissions of the as-prepared ZnO:Eu and $Y(OH)_3:Eu$ are shown in the supplementary **Figure 1**. It is observed the luminescence emission of ZnO:Eu is strong whereas that of $Y(OH)_3:Eu$ is weak as Y_2O_3 is amorphous at this temperature and the emissions are from the surface ions *i.e.* from weakly bonded Eu_2O_3 . Crystallization of Y_2O_3 starts only when annealed at higher temperatures and substitution of Y^{3+} by Eu^{3+} starts at this condition only. When Eu^{3+} ions occupy Y^{3+} site strong emissions could be obtained in such systems that is why the emission of heat-treated ZnO:Eu/ Y_2O_3 samples are intense. These results are similar to earlier reports [9] [24]-[26]. It is worth to mention that the peak positions of the heat-treated samples are found at 610 nm, these spectra are identical with heat-treated $Y_2O_3:Eu$ [9]. The substitution of Y^{3+} by Eu^{3+} are supported by XRD data that the unit cell volume of Y_2O_3 increased with the increase of heat-treatment temperatures. As the heat treatment temperatures increased more Eu^{3+} ions are leaving ZnO particles then migrate towards the Y_2O_3 lattice, where it feels an environment different from that of ZnO. That is why narrow and sharp Eu^{3+} emission lines at 610 nm could be observed in the luminescence emission spectra of annealed ZnO:Eu/ Y_2O_3 samples. **Figure 8** shows the comparisons of luminescence emission spectra of as-prepared ZnO:Eu and the ZnO:Eu nanoparticles covered with in yatria matrix (ZnO:Eu/ Y_2O_3), it is obvious that the luminescence emission of ZnO:Eu nanoparticles covered with in yatra matrix can be significantly improved its luminescence intensity compared to ZnO:Eu particles. The luminescence emission intensity of ZnO:Eu nanoparticles in yatra matrix is 10 times than the ZnO:Eu nanoparticles. This result will be useful for the further understanding of these systems of particles. It is expected the solubility of Eu^{3+} ions in ZnO are poor and most of the lanthanide ions may be on the surface of the ZnO particles or on the grain boundaries. These lanthanide ions migrates towards the amorphous environment of Y_2O_3 consequently reduces surface ions in ZnO. The surface lanthanide ions enhanced non-radiative transition leading weak luminescence emission, due to this ZnO:Eu covered with in Y_2O_3 have more intense compared to ZnO:Eu nanoparticles. For further confirmation of location of Eu^{3+} ions in ZnO:Eu/ Y_2O_3 nanoparticles the excitation spectra are taken by monitoring at 615 nm for as-prepared and heat-treated samples as shown in **Figure 9**. The pattern consists of a broad peak around 250 nm for the heat-treated samples which are the characteristics of Eu-O charge transfer band in Y_2O_3 lattice [1] [27]. Such Eu-O charge transfer band could not be observed in as-prepared ZnO:Eu/ Y_2O_3 nanocrystals but only the $f-f$ absorption band at longer wavelength could be observed. This simply confirms that in as-prepared sample the

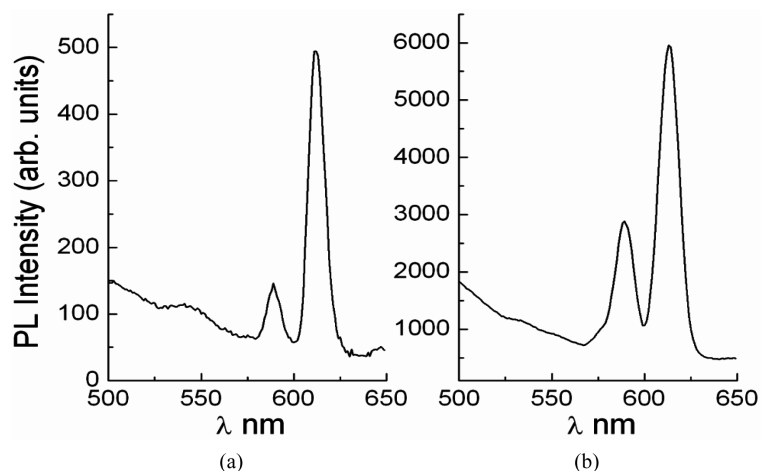


Figure 8. Photoluminescence emission spectra of (a) as-prepared ZnO:Eu nanoparticles and (b) ZnO:Eu nanoparticles covered with Y_2O_3 matrix (ZnO:Eu/ Y_2O_3) excited with $f-f$ transition 394 nm.

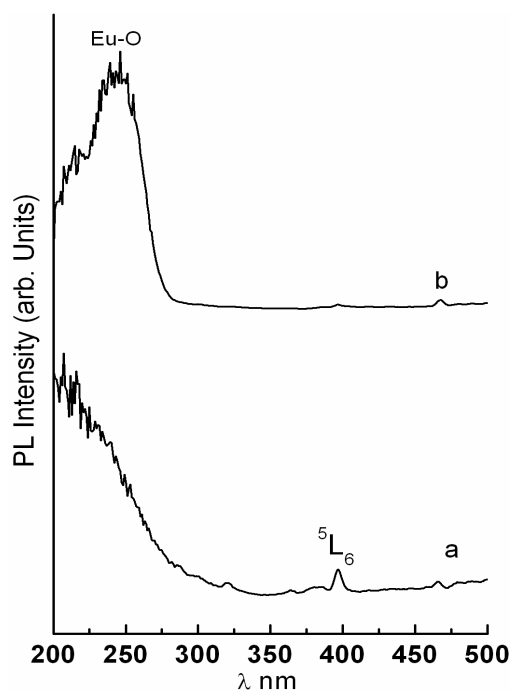


Figure 9. Excitation spectra of ZnO:Eu/ Y_2O_3 nanoparticles (a) as-prepared monitored at 615 nm and (c) 900°C monitored at 610 nm.

Eu^{3+} ions are adapted in the amorphous environment of Y_2O_3 , not forming the bond with Y^{3+} site. The above observations have revealed that there are significant numbers of surface Eu^{3+} ions on the ZnO nanoparticles and phase segregation of Eu^{3+} ions can be significantly reduced by incorporation by the Y_2O_3 matrix. The ratio of the integrated intensities of magnetic dipole transition $^5D_0 \rightarrow ^7F_2$ and electric dipole transition $^5D_0 \rightarrow ^7F_1$ transitions can be considered indicative of the asymmetry of coordination of Eu^{3+} ions [9].

Asymmetric ratio A_{21} for as-prepared ZnO:Eu/ Y_2O_3 nanoparticle is found to be 3.4 that of heat-treated at 500°C and 900°C are found to be 4.8 and 5.3 respectively. This simply indicating the that co-ordination of Eu-O could be improved for the annealed samples, the Eu^{3+} ions are leaving ZnO and making co-ordination with Y^{3+} . The co-ordinations of Eu-O are also increase with the increase of annealing temperature. But the result is contrary with ZnO:Eu systems, in these system the asymmetric ratio decreases with the increase of annealing tem-

peratures. From the above observations in the luminescence emissions of both the systems (ZnO:Eu and ZnO:Eu/Y₂O₃) it is evident that covering of ZnO:Eu nanoparticles in Y₂O₃ can significantly reduced phase segregation of Eu₂O₃ in these systems.

4. Conclusion

Nanocrystals of ZnO, Eu³⁺ doped ZnO (ZnO:Eu) and ZnO:Eu covered with in Y₂O₃ could be successfully prepared at low temperature by wet chemical method in polyethylene glycol medium. Luminescence emission of pure ZnO nanoparticles depends on their particle sizes. However, there is a significant reduction in the luminescence intensity of annealed ZnO:Eu compared with the as-prepared ZnO:Eu which can be attributed to the partial phase segregation of Eu³⁺ ions as well as the incorporation of Eu³⁺ ions in the grain boundaries leading to distorted environment. The phase segregation and the incorporation of Eu³⁺ ions at the grain boundaries can be significantly reduced by incorporating the ZnO:Eu nanoparticles in Y₂O₃.

Acknowledgements

The author awes Dr. R. S. Ningthoujam, Scientific Officer E, Chemistry Division of BARC, Mumbai for providing all the facilities of characterization, luminescence measurements and constant encouragement while preparing this manuscript. The author thanks DST New Delhi for providing financial assistance under DST Fast Tract Young Scientist Scheme (SR/FTP/PS-128/2011) during execution of this work and UGC New Delhi for providing financial assistance under UGC Start Up Grant with sanction No.F.20-1(25)/2012(BSR).

References

- [1] Blasse, G. (1994) Luminescent Materials. Springer, New York. <http://dx.doi.org/10.1007/978-3-642-79017-1>
- [2] Yen, W.M. and Shionoya, S. (1998) Phosphor Handbook. CRC Press, Boca Raton.
- [3] Hayashi, Y., Narahara, H., Uchida, T., Noguchi, T. and Ibuki, S. (1995) Photoluminescence of Eu-Doped ZnO Phosphors. *Japanese Journal of Applied Physics*, **34**, 1878. <http://dx.doi.org/10.1143/JJAP.34.1878>
- [4] Mardkovich, V.Z., Hayashi, H., Haemori, M., Fukumura, T. and Kawasaki, M. (2003) Discovery and Optimization of New ZnO-Based Phosphors Using a Combinatorial Method. *Advanced Functional Materials*, **13**, 519-524. <http://dx.doi.org/10.1002/adfm.200304335>
- [5] Ishizumi, A., Taguchi, Y., Yamamoto, A. and Kanemitsu, Y. (2005) Luminescence Properties of ZnO and Eu³⁺-Doped ZnO Nanorods. *Thin Solid Films*, **486**, 50-52. <http://dx.doi.org/10.1016/j.tsf.2004.11.229>
- [6] Yang, C., Cheng, S., Lee, H. and Chen, S. (2006) Effects of Phase Transformation on Photoluminescence Behavior of ZnO:Eu Prepared in Different Solvents. *Ceramics International*, **32**, 37-41. <http://dx.doi.org/10.1016/j.ceramint.2004.11.016>
- [7] Panatarani, C., Lenggoro, I.W. and Okuyama, K. (2004) The Crystallinity and the Photoluminescent Properties of Spraypyrolyzed ZnO Phosphor Containing Eu²⁺ and Eu³⁺ Ions. *Journal of Physics and Chemistry of Solids*, **65**, 1843-1847. <http://dx.doi.org/10.1016/j.jpccs.2004.06.008>
- [8] Singh, L.R., Ningthoujam, R.S., Sudarsan, V., Singh, S.D. and Kulshrestha, S.K. (2008) Probing of Surface Eu³⁺ Ions Present in ZnO:Eu Nanoparticles by Covering ZnO:Eu Core with Y₂O₃ Shell: Lu-Minescence Study. *Journal of Luminescence*, **128**, 1544-1550. <http://dx.doi.org/10.1016/j.jlumin.2008.02.013>
- [9] Singh, L.R., Ningthoujam, R.S., Sudersan, V., Srivastava, I., Singh, S.D., Dey, G.K. and Kulshrestha, S.K. (2008) Luminescence Study on Eu³⁺ Doped Y₂O₃ Nanoparticles: Particle Size, Concentration and Core-Shell Formation Effects. *Nanotechnology*, **19**, Article ID: 055201.
- [10] Singh, L.R., Ningthoujam, R.S. and Singh, S.D. (2009) Tuning of Ultra-Violet to Green Emission by Choosing Suitable Excitation Wavelength in ZnO: Quantum Dot, Nanocrystals and Bulk. *Journal of Alloys and Compounds*, **487**, 466-471. <http://dx.doi.org/10.1016/j.jallcom.2009.07.166>
- [11] JCPDS Card No 41-1105.
- [12] Wang, Z., Lin, C., Liu, X., Li, G., Luo, Y., Quan, Z., Xiang, H. and Lin, J. (2006) Tunable Photoluminescent and Cathodoluminescent Properties of ZnO and ZnO:Zn Phosphors. *Journal of Physical Chemistry B*, **110**, 9469-9476. <http://dx.doi.org/10.1021/jp057214t>
- [13] Van Dijken, A., Meulenkamp, E.A., Vanmaekelbergh, D. and Meijerink, A. (2000) The Kinetics of the Radiative and Nonradiative Processes in Nanocrystalline ZnO Particles upon Photoexcitation. *Journal of Physical Chemistry B*, **104**, 1715-1723. <http://dx.doi.org/10.1021/jp993327z>

- [14] Jia, W., Monge, K. and Fernandez, F. (2003) Energy Transfer from the Host to Eu^{3+} in ZnO. *Optical Materials*, **23**, 27-32. [http://dx.doi.org/10.1016/S0925-3467\(03\)00054-5](http://dx.doi.org/10.1016/S0925-3467(03)00054-5)
- [15] Bendre, B.S. and Mahamuni, S. (2004) Luminescence in ZnO Quantum Particles. *Journal of Materials Research*, **19**, 737-740. <http://dx.doi.org/10.1557/jmr.2004.19.3.737>
- [16] Ntwaeabirwam, O.M. and Holloway, P.H. (2005) Enhanced Photoluminescence of Ce^{3+} Induced by an Energy Transfer from ZnO Nanoparticles Encapsulated in SiO_2 . *Nanotechnology*, **16**, 865-872. <http://dx.doi.org/10.1088/0957-4484/16/6/042>
- [17] Li, D., Leung, Y.H., Djuricic, A.B., Liu, Z.T., Xie, M.H., Shi, S.L., Xu, S.J. and Chan, W.K. (2004) Different Origins of Visible Luminescence in ZnO Nanostructures Fabricated by the Chemical and Evaporation Methods. *Applied Physics Letters*, **85**, 1601-1604.
- [18] Kamat, P.V. and Patrick, B. (1992) Photophysics and Photochemistry of Quantized Zinc Oxide Colloids. *Journal of Physical Chemistry*, **96**, 6829-6834. <http://dx.doi.org/10.1021/j100195a055>
- [19] Vanheusden, K., Warren, W., Seager, C.H., Tallant, D.R., Voigt, J.A. and Gnade, B.E. (1996) Mechanisms behind Green Photoluminescence in ZnO Phosphor Powders. *Journal of Applied Physics*, **79**, 7983-7991. <http://dx.doi.org/10.1063/1.362349>
- [20] Halliburton, L.E., Giles, N.C., Graces, N.Y., Luo, M., Xu, C., Bai, L. and Boatner, L.A. (2005) Production of Native Donors in ZnO by Annealing at High Temperature in Zn Vapor. *Applied Physics Letters*, **87**, 172108-172111. <http://dx.doi.org/10.1063/1.2117630>
- [21] Djuricic, A.B., Leung, Y.H., Choy, W.C.H., Cheah, K.W. and Chan, W.K. (2004) Visible Photoluminescence in ZnO Tetrapod and Multipod Structures. *Applied Physics Letters*, **84**, 2635-2638. <http://dx.doi.org/10.1063/1.1695633>
- [22] Graces, N.Y., Wang, L., Bai, L., Giles, N.C., Halliburton, L.E. and Cantwell, G. (2002) Role of Copper in the Green Luminescence Crystals. *Applied Physics Letters*, **81**, 622-625. <http://dx.doi.org/10.1063/1.1494125>
- [23] Fonoberov, V.A., Alim, K.A., Balandin, A.A., Xiu, F. and Liu, J. (2006) Photoluminescence Investigation of the Carrier Recombination Processes in ZnO Quantum Dots and Nanocrystals. *Physical Review B*, **73**, 165317-165326. <http://dx.doi.org/10.1103/PhysRevB.73.165317>
- [24] Lima, S.A.M., Sigdi, F.A. and Davolos, M.R. (2003) Pechini's Solution as Precursor for Eu(III)-Containing ZnO Films. *Journal of Solid State Chemistry*, **171**, 287-290. [http://dx.doi.org/10.1016/S0022-4596\(02\)00178-0](http://dx.doi.org/10.1016/S0022-4596(02)00178-0)
- [25] Nageno, Y., Takebe, H., Morinaga, K. and Izumitani, T. (1994) Effect of Modifier Ions on Fluorescence and Absorption of Eu^{3+} in Alkali and Alkaline Earth Silicate Glasses. *Journal of Non-Crystalline Solids*, **169**, 288-294. [http://dx.doi.org/10.1016/0022-3093\(94\)90324-7](http://dx.doi.org/10.1016/0022-3093(94)90324-7)
- [26] Merino, R.P., Gallardo, A.C., Rocha, M.G., Calderon, I.H., Castano, V. and Rodriguez, R. (2001) Photoluminescence of TiO_2 : Eu^{3+} Thin Films Obtained by Sol-Gel on Si and Corning Glass Substrates. *Thin Solid Films*, **401**, 118-123. [http://dx.doi.org/10.1016/S0040-6090\(01\)01608-X](http://dx.doi.org/10.1016/S0040-6090(01)01608-X)
- [27] Vetrone, F., Boyer, J.C. and Capobianco, J.A. (2004) Yttrium Oxide Nanocrystals: Luminescent Properties and Applications. In: Nalwa, H.S., Ed., *Encyclopedia of Nanoscience and Nanotechnology*, Vol. 10, 725-765.